

Therapeutic distant organ effects of regional hypothermia during mesenteric ischemia-reperfusion injury

Rachel J. Santora, MD,^a Mihaela L. Lie, MD,^b Dmitry N. Grigoryev, MD, PhD,^c Omer Nasir, MD,^b Frederick A. Moore, MD,^a and Heitham T. Hassoun, MD,^{a,d} *Houston, Tex; and Baltimore, Md*

Introduction: Mesenteric ischemia-reperfusion injury (IRI) leads to systemic inflammation and multiple organ failure in clinical and laboratory settings. We investigated the lung structural, functional, and genomic response to mesenteric IRI with and without regional intraischemic hypothermia (RIH) in rodents and hypothesized that RIH would protect the lung and preferentially modulate the distant organ transcriptome under these conditions.

Methods: Sprague-Dawley rats underwent sham laparotomy or superior mesenteric artery occlusion (SMAO) for 60 minutes with or without RIH. Gut temperature was maintained at 15°-20°C during SMAO, and systemic normothermia (37°C) was maintained throughout the study period. At 6 or 24 hours, lung tissue was collected for (1) histology, (2) myeloperoxidase activity, (3) bronchoalveolar lavage (BAL) fluid protein concentrations, (4) lung wet/dry ratios, and (5) total RNA isolation and hybridization to Illumina's Sentrix BeadChips (>22,000 probes) for gene expression profiling. Significantly affected genes (false discovery rate <5% and fold change ≥1.5) were linked to gene ontology (GO) terms using MAPPFinder, and hypothermia-suppressed genes were further analyzed with Pubmatrix.

Results: Mesenteric IRI-induced lung injury, as evidenced by leukocyte trafficking, alveolar hemorrhage, and increased BAL protein and wet/dry ratios, and activated a proinflammatory lung transcriptome compared with sham. In contrast, rats treated with RIH exhibited lung histology, BAL protein, and wet/dry ratios similar to sham. At 6 hours, GO analysis identified 232 hypothermia-suppressed genes related to inflammation, innate immune response, and cell adhesion, and 33 hypothermia-activated genes related to lipid and amine metabolism and defense response. Quantitative real-time polymerase chain reaction validated select array changes in top hypothermia-suppressed genes lipocalin-2 (*lcn-2*) and chemokine ligand 1 (*CXCL-1*), prominent genes associated with neutrophil activation and trafficking.

Conclusions: Therapeutic hypothermia during SMAO provides distant organ protection and preferentially modulates the IRI-activated transcriptome in the rat lung. This study identifies potential novel diagnostic and therapeutic targets of mesenteric IRI and provides a platform for further mechanistic study of hypothermic protection at the cellular and subcellular level. (*J Vasc Surg* 2010;52:1003-14.)

Clinical Relevance: Visceral organ ischemia-reperfusion injury (IRI) is a common clinical problem in the settings of shock, sepsis, vascular surgery, and organ transplantation and is a particularly vexing problem in the repair of complex aortic aneurysms. IRI is associated with considerable patient morbidity and mortality, for which there are virtually no therapeutic options. It systematically causes local organ injury and dysfunction, systemic inflammation, and multiple organ failure. Clinical trials investigating the efficacy of pharmacologic blockade of individual downstream inflammatory mediators in critically ill patients have been largely unsuccessful, and such studies highlight the need for novel top-down approaches, such as gene expression profiling for biologic discovery, as well as application of broader therapeutic interventions, such as targeted hypothermia. In this study, we demonstrate the potential application of visceral cooling for distant organ protection during mesenteric IRI, identify broad changes in lung gene expression under these conditions, and have elucidated potential novel diagnostic and therapeutic targets for disease targeting.

From the Department of Surgery, The Methodist Hospital and Research Institute,^a and The Methodist DeBakey Heart & Vascular Center,^d Houston; and Departments of Surgery^b and Medicine,^c Johns Hopkins University School of Medicine, Baltimore.

Competition of interest: none.

Supported by grants from the American Vascular Association/American College of Surgeons Lifeline Award and National Institutes of Health (NIH) Grant K08HL089181.

Presented at the Thirty-fourth Annual Meeting of the Southern Association for Vascular Surgery in Paradise Island, Bahamas, January 20-23, 2010.

Correspondence: Heitham T. Hassoun, MD, Associate Professor of Cardiovascular Surgery, The Methodist Hospital Physician Organization, 6550 Fannin St, SM 1401, Houston, TX 77030 (e-mail: hhassoun@tmhs.org).

The editors and reviewers of this article have no relevant financial relationships to disclose per the JVS policy that requires reviewers to decline review of any manuscript for which they may have a competition of interest.

0741-5214/\$36.00

Copyright © 2010 by the Society for Vascular Surgery.

doi:10.1016/j.jvs.2010.05.088

Mesenteric ischemia-reperfusion injury (IRI) occurs in various clinical settings including shock, sepsis, and complex aortic surgery. It incites an inflammatory response associated with local gut dysfunction as well as neutrophil (polymorphonuclear [PMN]) activation and remote organ injury.¹⁻⁵ Numerous effectors have been implicated in this injury cascade, including cytokines, lipid mediators, nitric oxide, and cell adhesion molecules.⁶⁻¹⁰ Unfortunately, clinical trials investigating the efficacy of pharmacologic blockade of these various downstream inflammatory mediators in critically ill patients have been largely unsuccessful.^{11,12} It has become clear that a more thorough top-down approach to biologic discovery and implementation of interventions with broader therapeutic application are needed to improve outcomes in these clinical settings.

Therapeutic hypothermia is cytoprotective in various IRI models, and its protective mechanisms seem to go

beyond simply decreasing local metabolic demands during ischemia. Our prior work in rats demonstrated that regional intraischemic hypothermia (RIH) during superior mesenteric artery occlusion (SMAO) prevented reperfusion-induced intestinal mucosal injury and gut dysfunction, and RIH preferentially modulated the local oxidative stress transcriptional response during IRI.¹³ A subsequent clinical translational study demonstrated that cold visceral perfusion during thoracoabdominal aortic aneurysm (TAAA) repair improved survival in a subset of critically ill patients (ie, those who developed postoperative acute kidney injury) despite limited effects on the target organ.¹⁴ These findings suggest potential systemic or distant organ therapeutic effects of visceral cooling during TAAA repair. The aim of this laboratory investigation is to gain a better understanding regarding the effects of RIH on distant organ dysfunction during mesenteric IRI.

We investigated structural, functional, and transcriptional changes in the lung during mesenteric IRI in rats and hypothesized that regional gut hypothermia during SMAO protects the lung and preferentially modulates the IRI-activated transcriptome in the rat lung. To address this hypothesis, we used an established rodent model of mesenteric IRI that is known to cause local and distant organ injury and discovered lung microvascular injury and inflammation during mesenteric IRI that was mitigated by RIH. We then conducted global gene expression profiling of lung tissues during mesenteric IRI with and without RIH.

Using a candidate gene approach, we identified ischemia-specific changes in the lung transcriptome that are suppressed by hypothermia and that include prominent genes involved in inflammation and leukocyte chemotaxis. Select genes associated with neutrophil activation and that demonstrated major changes in expression (ie, CXCL-1 and Lipocalin-2) were validated by qualitative real-time reverse-transcription polymerase chain reaction (RT-PCR). To further identify key biologic processes involved in the distant organ protective effects of RIH, gene ontology (GO) analysis demonstrated early suppression of genes related to inflammation, cell adhesion, and the innate immune response, and activation of genes related to the defense response. This study identifies potential novel diagnostic and therapeutic targets and provides a platform for further study of the distant organ protective effects of regional hypothermia during mesenteric IRI.

MATERIALS AND METHODS

Animal care. All procedures were approved by the Johns Hopkins Animal Care and Use Committee and were consistent with the National Institutes of Health (NIH) *Guide for the Care and Use of Laboratory Animals*. Male Sprague-Dawley rats (~300 grams; Harlan Labs, Houston, Tex) were housed under pathogen-free conditions according to NIH guidelines at least 5 days before operative procedures. The rats were fasted 18 hours before surgery but were given free access to water. All procedures were performed using strict sterile techniques under general

anesthesia with inhaled isoflurane. Assessment of adequate anesthesia was obtained by paw and tail pinching.

Surgical procedures. The study design and animal model implemented for these experiments is shown in Fig 1. Each animal underwent a midline laparotomy with isolation of the superior mesenteric artery (SMA). For rats assigned to experimental IRI, a nontraumatic vascular clamp was placed on the SMA for 60 minutes with (IRI-H) or without (IRI) regional intraischemic hypothermia.

Our method for inducing regional hypothermia has been described in detail previously.¹³ Briefly, RIH was induced by exteriorizing the small intestine and placing it in moistened gauze between two cold compresses. A temperature probe was placed between the loops of bowel to monitor regional temperature, which was maintained at 15°-20°C during ischemia. At the end of the allotted ischemic time period, and just before clamp release, the cold compresses were removed and the intestine was irrigated with warm normal saline. The laparotomy incisions were then closed in two layers, and the rats recovered from anesthesia on warming blankets.

Control animals underwent the identical procedure with (Sham-H) and without (Sham) regional hypothermia. The small intestine was exteriorized for 60 minutes and placed between moistened gauze without placement of the vascular clamp on the SMA, as described above. Each animal was placed on a heating pad, and core temperature was maintained at 37°C during the entire procedure. The animals were sacrificed at 6 or 24 hours, and tissue was collected for the following studies described below.

Lung histology. Lung histologic injury was assessed by evaluation of architecture and evidence of neutrophil influx with hematoxylin and eosin (H&E) staining, as previously described.¹⁵ After completion of the treatment period, the right main stem bronchus was identified and cross-clamped. A tracheostomy was performed and 0.5% low-melting agarose was instilled into the left lung at a constant pressure of 25 cm H₂O, allowing for expansion of the lung parenchyma. The inflated lungs were fixed in 10% formalin for 48 hours and embedded in paraffin blocks. Paraffin-embedded sections (5 μm) were obtained and stained with H&E (Fisher Scientific, Pittsburgh, Pa). Representative samples were analyzed with light microscopy (original magnification ×40) for evidence of injury and neutrophil influx.

Myeloperoxidase assay. Whole lung tissue was homogenized using cell lysis buffer (Cell Signaling), and 50 μL of each sample was added to a 96-well plate and incubated with 100-μL of SureBlue TMB 1-Component Microwell Peroxidase (KPL, Gaithersburg, Md) at room temperature for 20 minutes. The reaction was terminated using 100 μL of 0.18 M sulfuric acid. The optical density was at 450 nm using a Kinetic Microplate Reader (Molecular Devices Corporation, Sunnyvale, Calif) spectrophotometer. Results are expressed as ng/mg protein.

Lung permeability. Bronchoalveolar lavage (BAL) protein concentration was performed as a surrogate for lung microvascular permeability. BAL fluid collection was obtained by delivering 3 mL of warm PBS by tracheotomy,

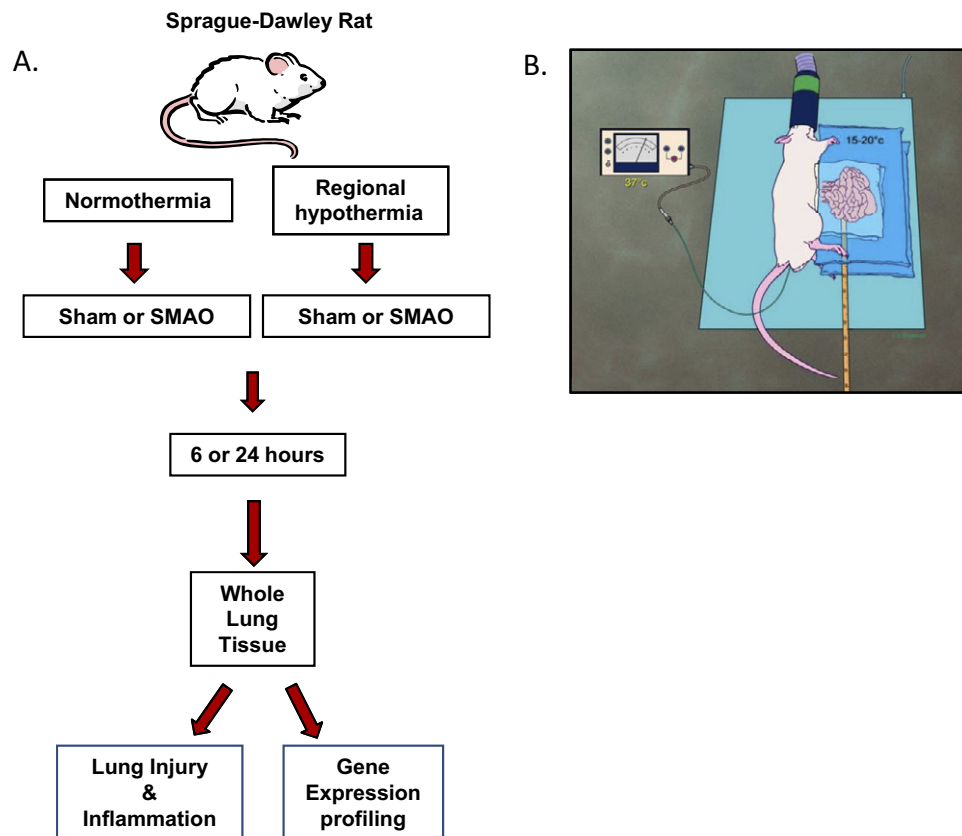


Fig 1. Experimental model. **A**, Sprague-Dawley rats underwent sham laparotomy or superior mesenteric artery occlusion (SMAO) for 60 minutes with and without regional hypothermia. After the allotted reperfusion time, 6 or 24 hours, the animals were sacrificed and whole lung tissue was collected. The collected tissue was analyzed for evidence of lung injury and inflammation, and total RNA was isolated from the lung for gene expression profiling. **B**, Regional intraischemic hypothermia (RIH) is illustrated. For animals selected to undergo RIH, the intestines were exteriorized and placed between two cold compresses. A temperature probe was used to monitor RIH, and animals were placed on a heating pad to maintain systemic normothermia (37°C).

and the recovered fluid was centrifuged at 1500 rpm at 4°C for 10 minutes. Protein concentration was measured using BCA total protein assay (Bio-Rad, Hercules, Calif) according to the manufacturer's protocol, and results are expressed as $\mu\text{g}/\text{mL}$.

Lung wet/dry ratio. As a surrogate for lung edema, lung tissues were obtained and wet weights determined before placing tissues in an oven at 60°C. After 48 hours, dry weights were measured and used to determine lung edema [(wet weight – dry weight)/dry weight].

Statistical analysis. For measurements of BAL protein and lung wet/dry ratios, data are expressed as means \pm standard error of the mean and were analyzed with one-way analysis of variance. Individual group means were compared with a Tukey multiple comparison test and *P* values <.05 were considered significant.

Microarray methods

Transcript profiling with Illumina oligonucleotide array. To identify potential IRI-specific distant organ transcriptional changes, total RNA from lung ($n =$

3/group) was isolated 6 or 24 hours after sham or SMAO with and without regional hypothermia. Total RNA was extracted using the Trizol Reagent method (Invitrogen, Carlsbad, Calif), and additional purification was performed on RNeasy columns (Qiagen, Valencia, Calif). The quality of total RNA samples was assessed using an Agilent 2100 Bioanalyzer (Agilent Technologies, Palo Alto, Calif). RNA samples were labeled according to the chip manufacturer's recommended protocols. In brief, for Illumina, 0.5 μg of total RNA from each sample was labeled by using the Illumina TotalPrep RNA Amplification Kit (Ambion, Austin, Tex) in a two-step process of complimentary DNA (cDNA) synthesis, followed by in vitro RNA transcription. Single-stranded RNA (cRNA) was generated and labeled by incorporating biotin-16-UTP (Roche Diagnostics GmbH, Mannheim, Germany), and 0.75 μg of biotin-labeled cRNA was hybridized (16 hours) to Illumina's Sentrix RatRef-12 v1 Expression BeadChip (>22,000 probes).

Sample quality control. The stringent quality control of the purity and integrity of the RNA was assessed

using standard criteria for RNA quality. The starting material was analyzed with the Agilent 2100 Bioanalyzer (Agilent Technology) that requires nanogram quantities of RNA. All RNA samples that were used for hybridization exhibited intact 28S and 18S ribosomal RNA on denaturing agarose gel electrophoresis; 260/280 nm absorbance readings for both total RNAs and biotin-cRNAs fall in the range of 1.8 to 2.1. Only samples with yields of in vitro transcribed RNA >750 ng were hybridized to the chips. After the chips were scanned, they were inspected for possible image artifacts.

Identification of significant transcriptional changes. The hybridization signals were analyzed using BeadStudio 1.5.0.34 software (Illumina Inc). The resulting digitized matrix was processed by modified for the Illumina platform approach described previously.¹⁶ Briefly, the significance (BeadStudio detection >0.95) of hybridization signals was tested, and “present” and “absent” transcripts were identified. The chip background and brightness was computed using high quartile and the entire set of “absent” hybridization signals, respectively. The expression data were stratified by experimental conditions and hybridization of each transcript was evaluated for each cluster. The transcripts determined to be “present” produced a signal at least twice as high as that of background in at least two of three hybridizations in any given group of rats were considered expressed.

The signal intensity values of these transcripts from each chip were increased by corresponding to a given chip background value (background adjustment) and divided by a chip brightness coefficient (normalization). The normalized data then were processed by Significance Analysis of Microarrays (SAM 2.20) using full permutation of three control and three IRI or IRI-H samples (720 permutations) without application of arbitrary restrictions.^{17,18} Genes with 1.5-fold change and false discovery rate (q value) of <5% were considered significantly associated with IRI.

Hierarchical clustering. Fold change values for individual IRI or IRI-H samples, or both, were derived by subtraction of average control expression (log₂ format) from corresponding experimental expressions (log₂ format). The 300 most variable significant genes were clustered based on a gene expression pattern similarity (Pearson correlation) using MeV software.

Validation of gene expression data. Quantitative real-time RT-PCR validation of selected candidate genes was conducted as previously described.^{19,20} Briefly, transcript levels of selected candidate genes in control and IRI-affected lung tissues were measured ($n = 3$ per condition) in 96-well microtiter plates with an ABI Prism 7700 Sequence Detector Systems (Perkin-Elmer/Applied Biosystems). Three TaqMan endogenous control genes (Gapdh, Actb, and Pglyk1) were used as internal controls for normalization. Primers and probes were purchased from Applied Biosystems Inc in a 20X mixture. All experimental protocols were based on the manufacturer’s recommendation using the TaqMan Gold

real-time RT-PCR Core Reagents Kit (Perkin-Elmer/Applied Biosystems, P/N 402876). Experimental parameters were 48°C for 30 minutes, followed by 40 cycles of 95°C for 15 seconds and 60°C for 1 minute. Relative gene expression was calculated using the $2^{-\Delta\Delta Ct}$ method, which generates fold-change values for mRNA transcript levels expressed in IRI-treated lung samples relative to sham-operated samples, as described previously.²⁰

GO and PubMatrix analysis. MAPPFinder, a tool that integrates gene expression data with GO data, was used to identify the significant biologic trends among the array data collected from each experimental group. Compatible files were prepared using a GenMAPP converting tool as we described previously.²¹ Significant bioprocesses were selected by choosing GO terms containing >5% of the total number of genes linked by MAPPFinder. The Z score >2 and first GO node >0 criteria were also applied as filtering conditions. The selected gene candidates were then searched against terms of interest related to acute lung injury including, “neutrophil,” “endothelium,” “epithelium,” and “pulmonary” terms in PubMed database using the PubMatrix automated literature search engine.²²

RESULTS

Lung morphology during mesenteric IRI. To assess potential structural changes in the lung after experimental IRI with and without hypothermia, H&E-stained sections of the lung were analyzed under light microscopy and representative sections are shown in Fig 2. IRI-treated rats demonstrated persistent neutrophil infiltration and focal alveolar hemorrhage, findings that were not present after sham, sham-H, or IRI-H. To quantify neutrophil influx, we measured myeloperoxidase (MPO) activity in all experimental groups. At 24 hours, there was a significant increase in MPO activity in IRI compared with sham controls (7.1 ± 0.4 vs 5.9 ± 0.3 , $P < .05$) during normothermia but no difference between IRI-H and sham-H (6.5 ± 0.4 vs 6.3 ± 0.4 , $P > .05$).

BAL protein during mesenteric IRI. The effect of RIH on pulmonary function during mesenteric IRI was evaluated by measuring changes in BAL protein concentrations ($\mu\text{g}/\text{mL}$) as a surrogate for microvascular permeability (Fig 3). At 24 hours, BAL protein concentration was increased in IRI-treated rats (665 ± 29) compared with sham (145 ± 24) and IRI-H (85 ± 58).

Lung weight/dry ratios during mesenteric IRI. To further evaluate the effect of RIH on pulmonary microvascular permeability, we measured weight/dry ratios as an indicator of pulmonary edema (Fig 4). Wet/dry ratios were increased in IRI compared with sham (1.17 ± 0.01 vs 1.21 ± 0.01 ; $P \leq .05$) and IRI-H (1.21 ± 0.01 vs 1.13 ± 0.001 , $P \leq .05$).

Gene expression changes in the lung during mesenteric IRI. Global gene expression profiling is a robust tool for identification of diagnostic and mechanism-related candidate genes. To evaluate the lung genomic response to mesenteric IRI with and without hypothermia, we con-

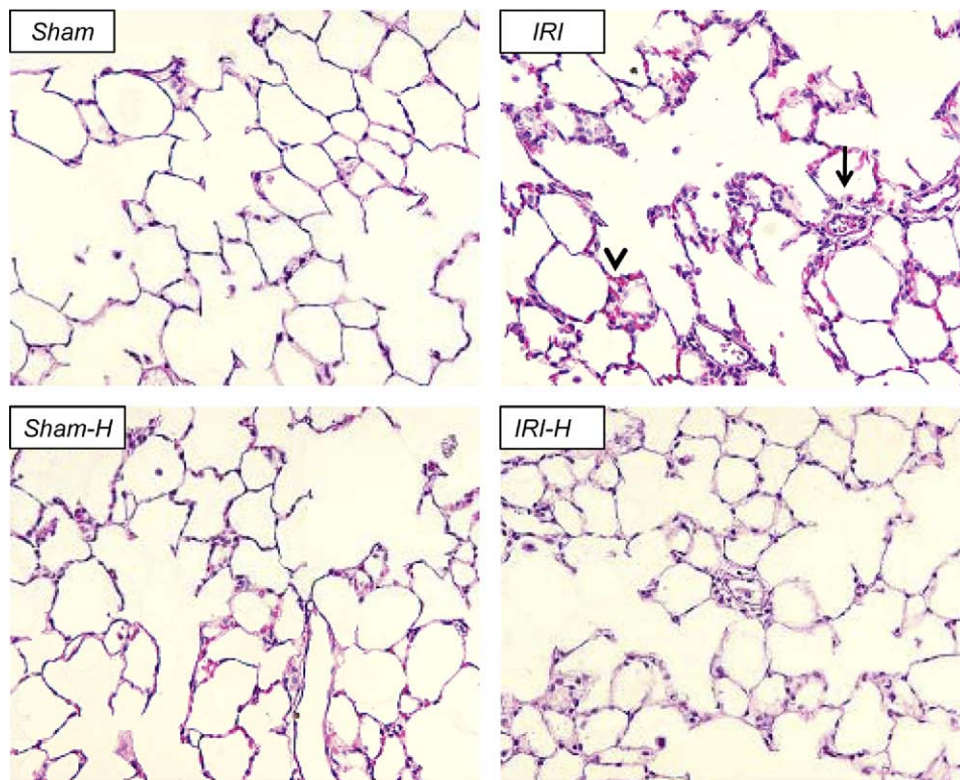


Fig 2. Effect of regional hypothermia on lung injury during mesenteric ischemia-reperfusion injury (*IRI*). Representative sections of lung tissue at 24 hours after superior mesenteric artery occlusion, with and without hypothermia (*H*) are shown. *IRI*-treated rats demonstrate increased neutrophil influx (*arrowhead*) and alveolar hemorrhage (*arrow*) not present in sham, sham-*H*, or *IRI-H* (hematoxylin and eosin stain; original magnification $\times 40$).

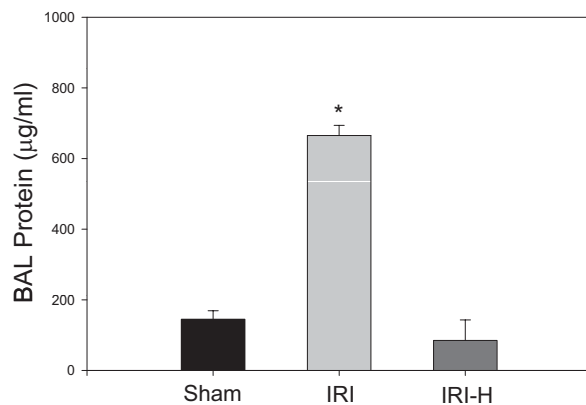


Fig 3. Effect of regional hypothermia (*H*) on lung bronchoalveolar lavage (*BAL*) protein during mesenteric ischemia-reperfusion injury (*IRI*). *BAL* protein concentration (mg/mL) at 24 hours was greater during *IRI* compared with sham and *IRI-H*. * $P \leq .05$, $n \geq 5$ rats/group. The *range bars* show the standard error of the mean.

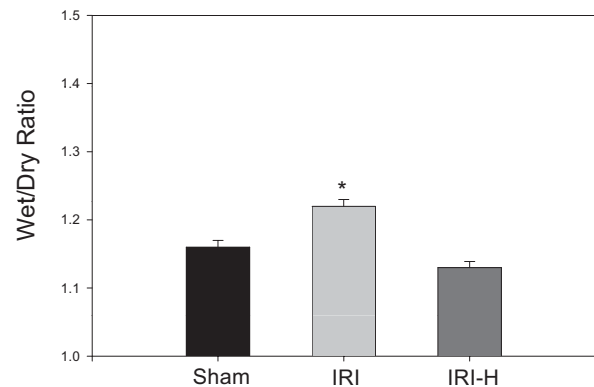


Fig 4. Effect of regional hypothermia on lung edema during mesenteric ischemia-reperfusion injury (*IRI*). Lung edema (wet/dry ratio) was increased in *IRI* compared with sham and *IRI-H*. * $P \leq .05$, $n \geq 5$ rats/group. The *range bars* show the standard error of the mean.

ducted global gene expression profiling of whole lung tissue obtained at 6 or 24 hours after sham, sham-*H*, *IRI*, and *IRI-H*. Total RNA was isolated from rat lungs ($n = 3$ /group) and hybridized to Illumina's Sentrix Expression

Bead chip ($>22,000$ probes). At 6 hours, SAM of expression profiles identified 437 lung genes with increased expression during *IRI* compared with sham, of which 205 genes were also activated in *IRI-H* treated groups. Therefore, of the *IRI*-induced genes, we identified 232 lung

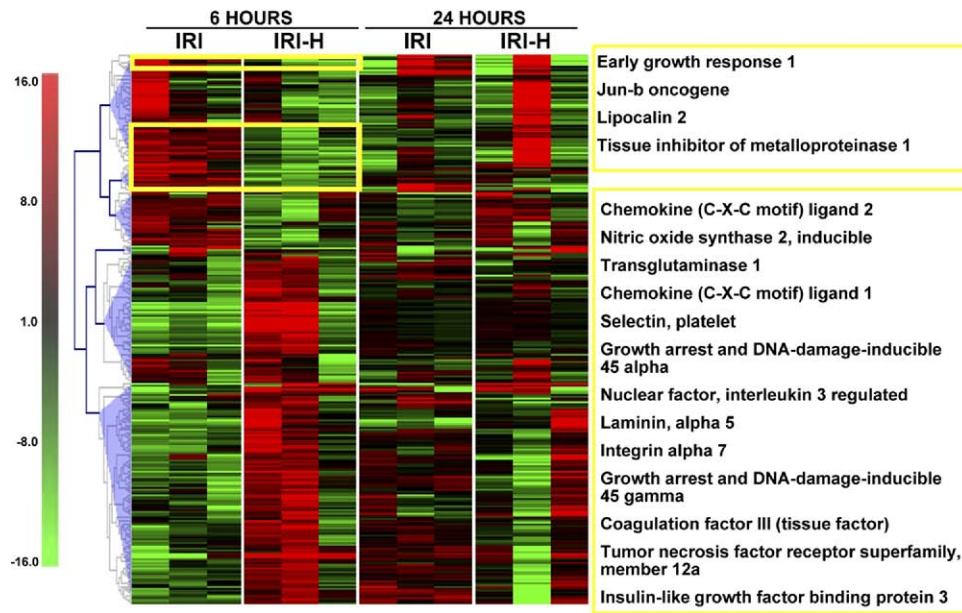


Fig 5. Hierarchic cluster analysis of lung gene expression during mesenteric ischemia-reperfusion injury (*IRI*) is shown at 6 and 24 hours. Each column represents an experimental condition of the corresponding lung sample. Hierarchic clustering using Pearson's correlation determined five major clusters (*blue triangles*), of which two clusters demonstrated clear differences in gene expression between *IRI* and *IRI-hypothermia (H)* at 6 hours. Genes from these clusters are highlighted with yellow rectangles and are listed on the right. *Red* indicates up-regulation, and *green* indicates down-regulation of gene expression with respect to corresponding controls.

candidate genes that were suppressed by regional hypothermia. In addition, we identified activation of 33 *IRI-H* specific genes. At 24 hours, there were only eight *IRI*-activated genes compared with sham, and there were no significant lung gene changes in the *IRI-H* treated group compared with sham controls.

To investigate potential differences in the lung genomic response to *IRI* and *IRI-H*, hierarchic cluster analysis of the most significantly affected genes identified groups of genes with similar as well as discordant expression patterns between the two treatment groups (Fig 5). The detailed analysis of the most differentially expressed genes between *IRI*- and *IRI-H*-treated animals are presented in Table I. Of note, several prominent genes related to leukocyte activation and trafficking, such as chemokine ligand 1 (*CXCL1*) and lipocalin-2 (*lcn-2*), were suppressed by hypothermia.

Validation of gene expression profiling findings.

To validate the results of our gene expression profiling studies, quantitative real-time RT-PCR measurements of selected genes was conducted using the TaqMan assay as described in Methods. The overall agreement between gene expression by microarray analysis and by the TaqMan assay was good, and the fold changes for the selected genes (*lcn-2* and *CXCL1*) are demonstrated in Fig 6. These genes were chosen for validation based on the most potentially relevant and representative significantly increased gene expression changes after *IRI*.

Identification of ischemia-specific biologic processes attenuated by intraischemic hypothermia.

Once significant differences in lung genomic responses between *IRI* and *IRI-H* were established, we focused on elucidation of potential mechanistic pathways unique to mesenteric *IRI*-induced lung structural and functional changes. Using MAPPFinder, we performed GO analysis of the 232 *IRI*-specific lung candidate genes that were suppressed by hypothermia and the 33 hypothermia-specific genes activated at 6 hours. GO analysis identified hypothermia-induced suppression of genes related to inflammation, cell adhesion, and innate immune response among others, and showed predominant activation of genes related to amine and lipid metabolism and defense response (Table II).

To further validate the biologic relevance of the lung candidate genes involved in these bioprocesses, a qualitative analysis of the *IRI* and hypothermia-specific transcripts was conducted using PubMatrix, an automated literature search engine (<http://pubmatrix.grc.nih.gov>). The 232 hypothermia-suppressed genes from the bioprocesses identified in the 6-hour GO analysis were matched against the terms "neutrophil," "endothelium," "epithelium," and "pulmonary" in the PubMed database. The most commonly cited genes related to these terms are presented in Table III and are listed according to weighted distribution between PMN or tissue based on the number of PubMed matches.

Table I. Top differentially expressed lung genes between ischemia-reperfusion injury (IRI) and IRI with hypothermia (IRI-H)

Gene title	Symbol	6 hours			24 hours		
		IRI	IRI-H	IRI-H/IRI Ratio	IRI	IRI-H	IRI-H/IRI ratio
Suppressed by hypothermia							
Actin alpha 1 skeletal muscle	<i>Acta1</i>	4.12	-1.44	0.17	1.11	1.61	1.45
Lipocalin 2	<i>Lcn2</i>	6.19	1.76	0.28	6.99	6.42	0.92
Chemokine (C-X-C motif) ligand 1	<i>Cxcl1</i>	7.45	2.26	0.30	1.65	4.54	2.76
Peripherin 1	<i>Prph1</i>	2.30	-1.40	0.31	-1.63	-1.11	1.47
LOC500721	<i>LOC500721</i>	2.45	-1.26	0.32	-1.42	1.11	1.57
Metallothionein	<i>Mt1a</i>	9.38	3.11	0.33	2.05	7.05	3.44
Chemokine (C-X-C motif) ligand 2	<i>Cxcl2</i>	4.67	1.69	0.36	1.19	2.54	2.13
LOC500720	<i>LOC500720</i>	2.64	-1.05	0.36	-1.46	1.25	1.82
Nitric oxide synthase 2 inducible	<i>Nos2</i>	4.10	1.66	0.41	1.18	1.95	1.66
Ring finger protein 30	<i>Rnf30</i>	3.05	1.27	0.42	1.00	3.36	3.37
Growth arrest and DNA-damage-inducible 45 gamma							
	<i>Gadd45g</i>	4.58	1.92	0.42	1.11	1.38	1.24
Ferredoxin 1	<i>Fdx1</i>	2.60	1.09	0.42	1.54	2.65	1.72
Hyaluronan synthase 1	<i>Has1</i>	2.42	1.11	0.46	1.33	1.35	1.01
Laminin alpha 5	<i>Lama5</i>	2.06	1.02	0.49	-1.04	2.18	2.27
Transglutaminase 1	<i>Tgm1</i>	3.45	1.72	0.50	1.29	1.71	1.32
Interferon-induced transmembrane protein 6	<i>Ifitm6</i>	3.86	2.68	0.69	10.06	4.94	0.49
Recovered by hypothermia							
Similar to 40S ribosomal protein S9	<i>LOC300278</i>	-4.35	1.04	4.53	-1.43	-1.54	0.93
Similar to 40S ribosomal protein S9	<i>LOC367102</i>	-2.62	1.20	3.15	-1.23	-1.40	0.88
Ribosomal protein S9	<i>Rps9</i>	-2.48	1.08	2.67	-1.24	-1.42	0.87
Cytochrome P450 family 2 subfamily e polypeptide 1							
	<i>Cyp2e1</i>	-3.14	-1.22	2.56	1.44	-1.74	0.40
Guanylate cyclase 1 soluble beta 3	<i>Gucylb3</i>	-2.49	-1.05	2.39	-1.02	-1.40	0.73
Chemokine (C-C motif) ligand 5	<i>Ccl5</i>	-2.41	-1.19	2.02	1.00	-1.54	0.65

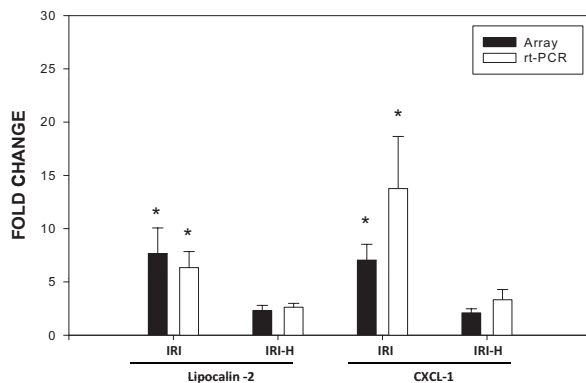


Fig 6. Expression of lipocalin-2 and chemokine ligand 1 (*CXCL-1*) genes in the lung by Illumina microarray and quantitative real-time reverse-transcription polymerase chain reaction (RT-PCR). The relative fold-change (at 6 hours) identified by microarray analysis (filled bars) and real-time RT-PCR (open bars) was calculated for IRI and IRI-H samples with respect to corresponding shams and is represented as mean \pm standard error of the mean. *Significant changes in gene expression between sham and treatment groups by either unpaired *t*-test (real-time RT-PCR) or significance analysis of microarrays (SAM; microarray). $P \leq .05$ or $q < 5\%$, respectively, $n \geq 3$ samples/group.

DISCUSSION

Mesenteric IRI is a common clinical condition in vascular surgical patients and is associated with significant

morbidity and mortality, for which there are virtually no therapeutic options. It promotes local synthesis and release of downstream inflammatory mediators that exacerbate gut injury and “prime” circulating neutrophils for enhanced superoxide anion production and subsequent remote organ injury.^{23,24} Complex thoracoabdominal aortic aneurysm (TAAA) repair results in obligatory mesenteric ischemia during repair of the visceral segment, and visceral organ IRI has been associated with distant organ injury, subsequent multiple organ failure (MOF), and death in clinical studies.^{25,26} In a recent prospective study of 10 patients undergoing TAAA repair, Feezor et al²⁷ identified adverse clinical outcome by blood leukocyte genomic and plasma proteomic responses after surgery. Using gene expression profiling and multiplex proteomic analysis, the authors identified time-dependent changes in gene expression that predicted subsequent organ dysfunction. This study highlights the potential utility of microarray analysis in preoperative risk assessment and as a potential tool to determine diagnostic and therapeutic targets of visceral IRI-induced MOF.

Surgical adjuncts to reduce the postoperative sequelae of visceral IRI during TAAA repair have focused on maintaining distal aortic perfusion and selective visceral cooling during repair of the visceral segment. Randomized comparisons of cold vs warm crystalloid and cold crystalloid vs cold blood perfusion have demonstrated the therapeutic benefits of visceral cooling for organ protection during IRI.^{28,29}

Table II. Gene ontology (GO) analysis of top differentially expressed lung genes between ischemia-reperfusion injury (IRI) and IRI with hypothermia (H)

Gene ontology ID	Gene ontology name	Changed genes (No.)	Measured genes (No.)	Changed genes (%)	Z score
Suppressed by hypothermia					
6928	Cell motility	11	88	12.5	4.352
6954	Inflammatory response	8	80	10.0	2.959
42127	Regulation of cell proliferation	9	108	8.33	2.528
7155	Cell adhesion	14	169	8.28	3.154
30154	Cell differentiation	10	130	7.69	2.391
6955	Immune response	16	230	6.96	2.619
9607	Response to biotic stimulus	17	269	6.32	2.279
Activated by hypothermia					
9308	Amine metabolism	4	122	3.28	3.924
6629	Lipid metabolism	4	182	2.20	2.886
6952	Defense response	4	250	1.60	2.142

In another large prospective study of 359 patients who underwent cold or warm blood visceral perfusion during TAAA repair, Hassoun et al¹⁴ demonstrated that although visceral cooling did not reduce the overall incidence of postoperative kidney injury during TAAA repair, it did improve survival in patients who developed renal failure.¹⁴ These findings suggest that regional hypothermia offers systemic protection during visceral IRI, although the exact mechanisms remain unclear.

In an effort to elucidate the therapeutic potential of regional hypothermia on distant organ inflammation and injury during mesenteric IRI, our laboratory has developed a rodent model of regional intraischemic hypothermia to study local and remote organ injury during SMAO. Early experimental studies using this model have shown that hypothermia confers local gut structural and functional protection by preserving mucosal integrity and improving intestinal transit during mesenteric IRI, and that RIH preferentially activates heme oxygenase-1 in the gut, while decreasing the expression of nuclear factor κ -B and deleterious inducible nitric oxide synthase.^{13,30} On the basis of these observations, our laboratory is now focused on the potential for therapeutic hypothermia to confer protection to distant organ sites during mesenteric IRI and to develop a better understanding of its modulating effects on the inflammatory response under these conditions.

Using a top-down approach, we conducted global gene expression profiling of rat lung obtained at 6 and 24 hours after mesenteric ischemia with and without RIH. To correlate genomic changes with structural and functional derangements in the lung, we assessed time-dependent changes in BAL protein concentration, wet/dry ratios, and lung histology in all experimental groups. Within 24 hours of mesenteric ischemia, there was a significant increase in BAL protein concentrations and wet/dry ratios, indicating increased pulmonary microvascular permeability and lung edema in IRI-treated animals as well as histologic evidence of alveolar damage and neutrophil trafficking. The structural and functional changes observed at 24 hours are likely preceded by changes in the proinflammatory transcriptome

that return to baseline within 24 hours. These observations suggest that IRI-induced transcriptional changes occur before obvious functional or structural changes. Furthermore, neither transcriptional nor structural changes were present in hypothermia-treated animals, suggesting prominent distant organ protection under these conditions.

After determining the IRI-specific lung molecular signature, we were able to identify and characterize the hypothermia-suppressed lung transcriptome and validated these findings with real-time RT-PCR. Using a bioinformatic-driven approach, we determined the relevant biologic processes associated with the alterations in the lung transcriptome during mesenteric IRI with or without RIH. GO analysis identified hypothermia-induced suppression of genes related to inflammation, cell adhesion, and the innate immune response, and showed activation of genes related to amine and lipid metabolism and the defense response. Interestingly, among the top hypothermia-suppressed genes are *CXCL-1*, *CXCL-2*, and *lipocalin-2*, which all code for proteins prominently associated with neutrophil trafficking and activation. The biologic relevance of these top suppressed genes was validated by using an automated literature search engine, PubMatrix (<http://pubmatrix.grc.nia.nih.gov>). The weighted distribution of the most commonly cited genes were matched to the terms "neutrophil" and tissue-specific components such as "epithelium" or "endothelium," thus allowing for future mechanism-based studies of the therapeutic potential of RIH focusing on its specific effects on leukocyte- or tissue-specific receptors.

Indeed, activation and migration of circulating neutrophils are central events in the development of acute lung injury.^{31,32} Chemokines are important mediators of neutrophil recruitment and activation in the lung in response to an inflammatory stimulus. CXCL-1 and CXCL-2 are glutamic acid-leucine-arginine (ELR+) chemokines that act through a shared G-protein-coupled receptor, CXCR2. Studies have highlighted the importance of CXCR2 ligand-mediated lung injury and have demonstrated that increased CXCL-1 and CXCL-2 expression parallels neutrophil se-

Table III. Qualitative analysis of hypothermia-suppressed genes using PubMatrix^a

Gene title	Gene symbol	PubMed search terms					Ratio PMN/tissue ^b	Distribution
		Neutrophil	Endothelium	Epithelium	Pulmonary			
Neutrophil cytosolic factor 1	<i>Ncf1</i>	44	0	0	2	44.00		
Neutrophil cytosolic factor 2	<i>Ncf2</i>	17	0	0	3	17.00		
Lipocalin-2	<i>Lcn2</i>	256	5	26	39	8.26		
Chemokine ligand 2	<i>Cxcl2</i>	664	44	88	463	5.03	PMN	
Chemokine ligand 1	<i>Cxcl1</i>	761	94	162	269	2.97		
Biregional cell adhesion molecule-related/down-regulated by oncogenes binding protein	<i>Boc</i>	72	7	23	57	2.40		
Chemokine ligand 3	<i>Ccl3</i>	248	55	76	249	1.89		
Lipopolysaccharide binding protein	<i>Lbp</i>	95	28	51	96	1.20	Even	
CD 14 Antigen	<i>Cd14</i>	658	300	381	533	0.97		
Tumor necrosis factor receptor superfamily 12 MAP kinase-activated protein kinase 2	<i>Tnfrsf1a</i>	19	8	13	17	0.90		
CSX-associated LIM	<i>Mapkapk2</i>	25	23	27	20	0.50	Tissue	
Signal transducer and activator of transcription 3	<i>Cal</i>	33	18	51	168	0.48		
Coagulation factor 3	<i>Stat3</i>	158	111	253	342	0.43		
Spermidine/spermine N1-acetyl transferase	<i>F3</i>	22	15	42	69	0.39		
Inhibitor of kappa B kinase beta	<i>Sat</i>	18	19	40	182	0.31		
Complement component 4 gene 2	<i>Ikbkb</i>	61	80	138	166	0.28		
Plasminogen activator tissue Desmin	<i>C4-2</i>	4	3	12	7	0.27		
Guanine deaminase	<i>Plat</i>	10	19	19	24	0.26		
Prostaglandin-endoperoxide synthase 2	<i>Des</i>	630	755	1663	3266	0.26		
Period homolog 1	<i>Gda</i>	8	9	22	95	0.26		
NAD(P)H dehydrogenase quinone 1	<i>Ptgs2</i>	397	605	1046	1139	0.24		
Ectonucleotide pyrophosphatase/phosphodiesterase 2	<i>Per1</i>	2	1	8	18	0.22		
Runt-related transcription factor 1	<i>Enpp2</i>	2	2	8	10	0.20		
Gap junction membrane channel protein alpha 1	<i>Runx1</i>	12	34	38	10	0.17		
Kirsten rat sarcoma viral oncogene homologue 2 (active)	<i>Gjal</i>	2	5	10	8	0.13		
Vasodilator-stimulated phosphoprotein	<i>Kras2</i>	25	44	152	265	0.13		
Secreted phosphoprotein 1	<i>Vasp</i>	13	50	54	21	0.13		
Tissue inhibitor of metalloproteinase 1	<i>Spp1</i>	22	43	137	79	0.12		
Matrix Gla protein	<i>Timp1</i>	5	13	28	35	0.12		
Oxidized low-density lipoprotein (lectin-like) receptor 1	<i>Mgp</i>	5	17	34	36	0.10		
Elongation factor RNA polymerase II	<i>Oldr1</i>	3	16	15	1	0.10		
Neurturin	<i>Ell</i>	2	3	20	74	0.09		
P450 (cytochrome) oxidoreductase	<i>Nrtm</i>	1	1	12	1	0.08		
Glutathione peroxidase 2	<i>Por</i>	5	18	49	124	0.07		
Activating transcription factor 4	<i>Gpx2</i>	1	0	14	9	0.07		
Kruppel-like factor 5	<i>Atf4</i>	1	7	14	12	0.05		
	<i>Klf5</i>	1	7	20	4	0.04		

Table III. Continued

Gene title	Gene symbol	PubMed search terms					Ratio PMN/tissue ^b	Distribution
		Neutrophil	Endothelium	Epithelium	Pulmonary			
Insulin-like growth factor 1 receptor	<i>Igf1r</i>	7	59	158	161	0.03		
Hyaluronan synthase 1	<i>Has1</i>	1	12	22	17	0.03		
Forkhead box A2	<i>Foxa2</i>	1	3	45	61	0.02		
Wingless-related MMTV integration site 4	<i>Wnt4</i>	0	1	26	5	0.04		
Solute carrier family 7 (cationic amino acid transporter y+ system) member 1	<i>Slc7a1</i>	0	12	11	5	0.04		
Tumor-associated protein 1 (Slc7a5)	<i>Slc7a5</i>	0	6	13	13	0.05		
Procollagen type VII alpha 1	<i>Col7a1</i>	0	0	13	0	0.08		
Laminin alpha 5	<i>Lama5</i>	0	2	10	4	0.08		
Low-density lipoprotein receptor-related protein 6	<i>Lrp6</i>	0	0	10	4	0.10		
Huntingtin-associated protein 1 (Hap1) transcript variant 2	<i>Hap1</i>	0	2	7	13	0.11		
Surfactant-associated protein B	<i>Sftpb</i>	0	0	7	48	0.14		

PMN, Polymorphonuclear.

^aGenes that had at least 10 hits in one category were retained.

^bFor calculation of PMN/tissue ratio, zeroes were substituted with 1.

questration and progressive lung injury.^{33,34} In our current study, we identified *CXCL-1* and *CXCL-2* among the top lung candidate genes suppressed by hypothermia, and based on these observations, note that suppression of CXCR-2 ligand-mediated events may confer the protective effect of RIH on distant organ dysfunction.

We also identified and validated hypothermia-induced suppression of lipocalin-2, also known as lipocalin-associated MMP-9 or NGAL. Lipocalins are small, secreted proteins that form complexes with other macromolecules, including neutrophil gelatinase, to form NGAL, which consists of a stable complex between lipocalin and MMP-9. MMPs are preformed granules stored in mature neutrophils that are released in response to chemokine stimulation and are important in extracellular matrix degradation, tissue destruction, and cellular migration.^{35,36} Clinical studies have implicated MMPs, particularly MMP-8 and MMP-9, as mediators of pulmonary inflammation in acute and chronic pulmonary disease states.³⁷ In our study, we found early suppression of lung lipocalin-2 in RIH-treated animals, making it an attractive candidate for further investigation as a potential mediator of hypothermia-induced lung protection.

A potential limitation of our study is the absence of gene expression profiling of the postischemic intestine. Without these data, it is difficult to conclude if regional hypothermia modulates the lung transcriptome in a unique fashion or if the observed gene expression changes in the lung parallel those in the gut. We identified top hypothermia-suppressed lung genes as those related to neutrophil trafficking and activation, which may also be dampened in the gut as well.

Furthermore, our study used profound regional hypothermia (15°-20°C) to achieve distant organ protection, which may have deleterious tissue consequences later. The effects of more moderate hypothermia on both local and distant organ dysfunction are largely unknown and need further investigation. Another potential confounding factor is the use of topical cooling to achieve regional hypothermia. Clinical studies examining the utility of regional hypothermia have achieved this by perfusing cold blood or saline through the organ of interest. In our model, only topical hypothermia was used, and we therefore did not monitor the potential hemodynamic effects of using cold perfusate to achieve regional hypothermia. The potential hemodynamic consequences of using a cold perfusate would provide useful information for translation into a clinical model.

CONCLUSIONS

Clinical and experimental studies have demonstrated the promise of hypothermia as a rescue strategy after planned and unplanned ischemic events. Therapeutic hypothermia is a well-accepted postresuscitation strategy to reduce neurologic injury, improve myocardial function, and improve overall survival in patients with return of spontaneous circulation after out-of-hospital cardiac arrest. In an effort to optimize the therapeutic benefit of hypothermia, preliminary studies are establishing the optimal duration, target temperature, rate, and means of cooling.³⁸⁻⁴⁰ Although a large body of evidence supports the beneficial effects of systemic hypothermia, studies regarding use of hypothermia as a focused strategy for in vivo organ protection have been limited. Using an established

model of rodent SMAO, we have identified deleterious lung structural and functional changes during IRI that were mitigated by regional inraischemic hypothermia. Furthermore, RIH preferentially modulates the IRI-activated lung transcriptome by down-regulation of select proinflammatory genes and leukocyte chemoattractants. This study identifies potential novel diagnostic and therapeutic targets and provides a platform for further study of the distant organ protective effects of regional hypothermia during mesenteric IRI.

We would like to acknowledge Tonya Watkins and Chris Cheadle of the Johns Hopkins Bayview Medical Center Lowe Family Genomics Core for their expert technical assistance with the RT-PCR and microarray analyses.

AUTHOR CONTRIBUTIONS

Conception and design: HH
Analysis and interpretation: RS, DG, FM, HH
Data collection: ML, RS, DG, ON
Writing the article: RS, DG, HH
Critical revision of the article: RS, ML, DG, ON, FM, HH
Final approval of the article: RS, ML, DG, ON, FM, HH
Statistical analysis: ML, RS, DG, HH
Obtained funding: HH
Overall responsibility: HH

REFERENCES

- Dewar D, Moore FA, Moore EE, Balogh Z. Postinjury multiple organ failure. *Injury* 2009;40:912-8.
- Hassoun HT, Kone BC, Mercer DW, Moody FG, Weisbrodt NW, Moore FA. Postinjury multiple organ failure: the role of the gut. *Shock* 2001;15:1-10.
- Wattanasirichaigoon S, Menconi MJ, Delude RL, Fink MP. Effect of mesenteric ischemia and reperfusion or hemorrhagic shock on intestinal mucosal permeability and ATP content in rats. *Shock* 1999;12:127-33.
- Davidson MT, Dietch EA, Lu Q, Osband A, Feketeova E, Nemeth ZH, et al. A study of the biologic activity of trauma-hemorrhagic shock mesenteric lymph over time and the relative role of cytokines. *Surgery* 2004;136:32-41.
- Koike K, Moore EE, Moore FA, Read RA, Carl VS, Banerjee A: Gut ischemia/reperfusion produces lung injury independent of endotoxin. *Crit Care Med* 1994;22:1438-1444.
- Welborn MB 3rd, Douglas WG, Abouhame Z, Auffenburg T, Abouhamze AS, Baumhofer J, et al. Visceral ischemia-reperfusion injury promotes tumor necrosis factor (TNF) and interleukin-1 (IL-1) dependent organ injury in the mouse. *Shock* 1996;6:171-6.
- Grotz MR, Deitch EA, Ding J, Xu D, Huang Q, Regel G. Intestinal cytokine response after gut ischemia: role of gut barrier failure. *Ann Surg* 1999;229:478-86.
- Diebel LN, Liberati DM, Lucas CE, Ledgerwood AM. Systemic not just mesenteric lymph causes neutrophil priming after hemorrhagic shock. *J Trauma* 2009;66:1625-31.
- Breithaupt-Faloppa AC, Vitoretti LB, Coelho FR dos Santos Franco AL, Domingos HV, Sudo-Hayashi LS, Oliveira-Filho RM, et al. Nitric oxide mediates lung vascular permeability and lymph-borne IL-6 after an intestinal ischemic insult. *Shock*. 2009;32:55-61.
- Seal JB, Gewertz BL. Vascular dysfunction in ischemia-reperfusion injury. *Ann Vasc Surg* 2005;19:572-84.
- Huber TS, Gaines GC, Welborn MB 3rd, Rosenberg JJ, Seeger JM, Moldawer LL. Anticytokine therapies for acute inflammation and the systemic inflammatory response syndrome: IL-10 and ischemia/reperfusion injury as a new paradigm. *Shock* 2000;13:425-34.
- Minnich DJ, Moldawer LL. Anti-cytokine and anti-inflammatory therapies for the treatment of severe sepsis: progress and pitfalls. *Proc Nutr Soc*. 2004;63:437-41.
- Hassoun HT, Kozar RA, Kone BC, Safi HJ, Moore FA. Intraischemic hypothermia differentially modulates oxidative stress proteins during mesenteric ischemia/reperfusion. *Surgery* 2002;132:369-76.
- Hassoun HT, Miller CC 3rd, Huynh TT, Estrera AL, Smith JJ, Safi HJ. Cold visceral perfusion improves early survival in patients with acute renal failure after thoracoabdominal aortic aneurysm repair. *J Vasc Surg* 2004;39:506-12.
- Hassoun HT, Grigoryev DN, Lie ML, Liu M, Cheadle C, Tuder RM, et al. Ischemic acute kidney injury induces a distant organ functional and genomic response distinguishable from bilateral nephrectomy. *Am J Physiol Renal Physiol* 2007;293:F30-40.
- Grigoryev DN, Mathai SC, Fisher MR, Gargis RE, Zaiman AL, Houstens-Harris T, et al. Identification of candidate genes in scleroderma-related pulmonary arterial hypertension. *Transl Res* 2008;151:197-207.
- Tusher VG, Tibshirani R, Chu G. Significance analysis of microarrays applied to the ionizing radiation response. *Proc Natl Acad Sci U S A* 2001;98:5116-21.
- Larsson O, Wahlestedt C, Timmons JA. Considerations when using the significance analysis of microarrays (SAM) algorithm. *BMC Bioinformatics* 2005;6:129.
- Li J, Grigoryev DN, Ye SQ, Thorne L, Schwartz AR, Smith PL, et al. Chronic intermittent hypoxia up-regulates genes of lipid biosynthesis in obese mice. *J Appl Physiol* 2005;99:1643-8.
- Ma SF, Grigoryev DN, Taylor AD, Nonas S, Sammani S, Ye SQ, et al. Bioinformatic identification of novel early stress response genes in rodent models of lung injury. *Am J Physiol Lung Cell Mol Physiol* 2005;289:L468-77.
- Grigoryev DN, Finigan JH, Hassoun P, Garcia JG. Science review: searching for gene candidates in acute lung injury. *Crit Care* 2004;8:440-7.
- Becker KG, Hosack DA, Dennis G, Jr., Lempicki RA, Bright TJ, Cheadle C, et al. PubMatrix: a tool for multiplex literature mining. *BMC Bioinformatics* 2003;4:61.
- Hassoun HT, Fischer UM, Attuwaybi BO, Moore FA, Safi HJ, Allen SJ, Cox CS Jr. Regional hypothermia reduces mucosal NF-kappa B and PMN priming via gut lymph during canine mesenteric ischemia/reperfusion. *J Surg Res*. 2003;115:121-6.
- Moore EE, Moore FA, Franciose RJ, Kim FJ, Biffi WL, Banerjee A. The postischemic gut serves as a priming bed for circulating neutrophils that provoke multiple organ failure. *J Trauma* 1994;37:881-7.
- Harward TR, Welborn MB, Martin TD, Flynn TC, Huber TS, Moldawer LL, et al. Visceral ischemia and organ dysfunction after thoracoabdominal aortic aneurysm repair. A clinical and cost analysis. *Ann Surg* 1996;6:729-36.
- Welborn MB, Oldenburg HS, Hess PJ, Huber TS, Martin TD, Rauwerda JA, et al. The relationship between visceral ischemia, proinflammatory cytokines, and organ injury in patients undergoing thoracoabdominal aortic aneurysm repair. *Crit Care Med* 2000;28:3191-7.
- Feezor RJ, Baker HV, Wenzhong X, Lee A, Huber TS, Mindrinos M, et al. Genomic and proteomic determinants of outcome in patients undergoing thoracoabdominal aortic aneurysm repair. *J Immunol* 2004;172:7103-09.
- Koksoy C, LeMaire SA, Curling PE, Raskin SA, Schmittling ZC, Conklin LD, et al. Renal perfusion during thoracoabdominal aortic operations: cold crystalloid is superior to normothermic blood. *Ann Thorac Surg* 2002;73:730-8.
- LeMaire SA, Jones MM, Conklin LD, Carter SA, Criddell MD, Wang XL, et al. Randomized comparison of cold blood and cold crystalloid renal perfusion for renal protection during thoracoabdominal aortic aneurysm repair. *J Vasc Surg* 2009;49:11-9.
- Attuwaybi BO, Hassoun HT, Zou L, Kozar RA, Kone BC, Weisbrodt, et al. Hypothermia protects against gut ischemia/reperfusion-induced impaired intestinal transit by inducing heme oxygenase-1. *J Surg Res* 2003;115:48-55.
- Reutershan J, Ley K. Bench-to-bedside review: acute respiratory distress syndrome-how neutrophils migrate into the lung. *Critical Care* 2004; 8:453-61.

32. Abraham E. Neutrophils and acute lung injury. *Crit Care Med* 2003;31: S195-9.
33. Belperio JA, Keane MP, Burdick MD, Gomperts BN, Xue YY, Hong K, et al. CXCR2/CXCR2 ligand biology during lung transplant ischemia-reperfusion injury. *J Immunol*. 2005;175:6931-9.
34. Belperio JA, Keane MP, Burdick MD, Londhe V, Xue YY, Li K, et al. Critical role for CXCR2 and CXCR2 ligands during the pathogenesis of ventilator-induced lung injury. *J Clin Invest* 2002;110:1703-16.
35. Starckx PE, Van Den Steen AW, Van Damme J, Opdenakker G. Neutrophil gelatinase B and chemokines in leukocytosis and stem cell mobilization. *Leuk Lymphoma* 2002;43:233-41.
36. Opdenakker G, Van den Steen PE, Dubois B, Nelissen I, Van Collie E, Masure S, et al. Gelatinase B functions as regulator and effector in leukocyte biology. *J Leukoc Biol* 2001;69:851-9.
37. Hartog CM, Wermelt JA, Sommerfeld CO, Eichler W, Dalhoff K, Braun J. Pulmonary matrix metalloproteinase excess in hospital-acquired pneumonia. *Am J Respir Crit Care Med* 2003;167: 593-8.
38. Holzer AJ, Herkner H, Mullner M. Hypothermia for neuroprotection in adults after cardiopulmonary resuscitation. *Cochrane Database Syst Rev* 2009;CD004128.
39. Nolan JP, Morley PT, Hoek TL and Hickey RW. Therapeutic hypothermia after cardiac arrest. An Advisory Statement by the Advanced Life Support Task Force of the International Liaison Committee on Resuscitation. *Circulation* 2003;108:118-21.
40. Alam HB, Duggan M, Li Y, Spanilas K, Liu B, Tabbara M, et al. Putting life on hold—for how long? Profound hypothermic cardiopulmonary bypass in a swine model of complex vascular injuries. *J Trauma* 2008; 64:912-22.

Submitted Mar 19, 2010; accepted May 16, 2010.